



City Research Online

City, University of London Institutional Repository

Citation: Mahmoud, M., Alkhedher, M., Ramadan, M., Pullen, K. R., Olabi, A-G. & Naher, S. (2022). Experimental investigation into the potential of using a shallow ground-cooled condenser in Lebanon. *Energy Conversion and Management*, 264, 115729. doi: 10.1016/j.enconman.2022.115729

This is the accepted version of the paper.

This version of the publication may differ from the final published version.

Permanent repository link: <https://openaccess.city.ac.uk/id/eprint/28219/>

Link to published version: <https://doi.org/10.1016/j.enconman.2022.115729>

Copyright: City Research Online aims to make research outputs of City, University of London available to a wider audience. Copyright and Moral Rights remain with the author(s) and/or copyright holders. URLs from City Research Online may be freely distributed and linked to.

Reuse: Copies of full items can be used for personal research or study, educational, or not-for-profit purposes without prior permission or charge. Provided that the authors, title and full bibliographic details are credited, a hyperlink and/or URL is given for the original metadata page and the content is not changed in any way.

City Research Online:

<http://openaccess.city.ac.uk/>

publications@city.ac.uk

Experimental investigation into the potential of using a shallow ground-cooled condenser in Lebanon

Montaser Mahmoud^{1,2}, Mohammad Alkhedher³, Mohamad Ramadan^{2,4*}, Keith Pullen¹, Abdul-Ghani Olabi^{5,6}, Sumsun Naher¹

¹Department of Engineering, School of Mathematics, Computer Science and Engineering, City, University of London, UK

²Lebanese International University, PO Box 146404 Beirut, Lebanon

³Mechanical Engineering Department, Abu Dhabi University, United Arab Emirates

⁴International University of Beirut, PO Box 146404 Beirut, Lebanon

⁵Sustainable and Renewable Energy Engineering, University of Sharjah, Sharjah, UAE

⁶Mechanical Engineering and Design, Aston University, School of Engineering and Applied Science, Aston Triangle, Birmingham, B4 7ET, UK

Abstract

The aim of this paper is to investigate the potential of using shallow geothermal energy in Lebanon for cooling a power cycle. The study includes ground temperature measurement, operating system management, and pressure drop assessment. Temperatures were monitored at six positions underground reaching to a depth of 2 m in Bekaa-Lebanon during the whole of 2020. The temperature sensors were placed at depths of 0.3, 0.6, 1, 1.3, 1.6, and 2 m underground. At 2 m depth, the ground temperature showed high stability with an annual temperature difference of 7°C, while that of high and low ambient temperatures were 40°C and 33°C, respectively. Based on the comparison between ambient and ground temperatures, the ground cooling system can operate 207 days/year partially with full operations of 51 days. This shows that shallow geothermal energy has a great potential to activate a ground-based cooling system in this region. However, to avoid heat accumulation, use of another heat exchanger is recommended to support the ground cooling system. This heat exchanger can also provide coolth compensation when the power cycle is turned

off. The pressure drop inside the heat exchangers was found to be highly significant, hence, it was essential to add an intermediate water loop between the power cycle and the ground loop.

Keywords: Shallow geothermal energy, ground temperature, ground heat exchanger, ground-cooled condenser, power generation.

Nomenclature	
\dot{m}	mass flow rate (kg/s)
ΔP	pressure drop (kPa)
D	diameter (m)
f	friction coefficient
h	enthalpy (kJ/kg)
L	length (m)
η	efficiency
Q	volumetric flow rate (m ³ /s)
Re	Reynold's number
T	temperature (°C)
t	time (hr)
v	velocity (m/s)
W	power (kW)
ρ	density (kg/m ³)
<i>Abbreviations</i>	
DCV	directional control valve
DGC	direct ground cooling
EES	Engineering Equation Solver
GCS	ground cooling system
GE	geothermal energy
GHE	ground heat exchanger
GPP	geothermal power plant

I-DGC	indirect ground cooling
ORC	organic Rankine cycle
RES	renewable energy sources
<i>Subscripts</i>	
f	working fluid
g	ground
p	pump
t	turbine

1. Introduction

Renewable energy sources (RES) are considered to be the leading contenders for developments of energy systems that reduce or eliminate the use of fossil fuels and thereby decreasing their environmental impacts [1]. However, RES are usually characterized by their stochastic and intermittent natures such as solar [2] and wind [3] energies. This imposes a need to incorporate energy storage systems in order to mitigate fluctuations and provide continuous supply [4, 5]. Such systems may also have some impacts on the environment and so making RES-based systems not perfectly green. For these reasons, geothermal energy (GE) can be considered as one of the most attractive energy sources [6, 7]. Compared to RES, it is remarkably stable since it is not affected by immediate ambient air changes. GE also encourages the adoption of ideal green systems because the ground can be used as a thermal energy storage medium for other RES such as storing the excess of solar energy in boreholes [8, 9]. One of the most frequent hybridizations is the solar assisted ground source heat pump [10, 11]. Such hybrid systems are highly recommended to avoid large ground loop installations and thermal imbalance [12].

GE is mainly classified into two types: deep [13, 14] and shallow [15, 16]. There is a huge difference between these types since the former utilizes hot geothermal fluid while the latter is based on exchanging heat with the ground via shallow loops. Deep GE can be used to provide heating or activate a power cycle for electricity generation. Geothermal power plants (GPPs) can be found in three forms: dry steam [17, 18], flash [19, 20], and binary [21, 22] cycles. Dry steam GPP is the oldest type such that the geothermal fluid is available in the form of steam only which can be harnessed to drive a turbine-generator. The flash cycle could be used when the geothermal fluid is a mixture of steam and water. The fluid will pass through a flash separator before entering the turbine. The latest version of GPPs is the binary cycle which allows the geothermal fluid to pass through a heat exchanger to heat up another working fluid. GPPs have been also developed to cope with advanced types of applications such as hydrogen production [23, 24]. In shallow GE systems, ground loops are used to provide heating or cooling. Open ground loops are installed when there is enough amount of shallow water [25, 26]. However, ground heat exchangers (GHEs) are used more frequently since they are based on extracting/releasing heat from/to the ground [27, 28]. GHEs can be mainly installed vertically [29, 30] or horizontally [31, 32] depending on the available shallow geothermal conditions. There are two types of shallow GE systems: earth air heat exchanger [33, 34] and ground source heat pump [35, 36].

One of the latest developments of GE systems is the use of a ground-cooled condenser as shown in Figure 1 [37, 38]. This has shown a great potential to use shallow geothermal energy for cooling power cycles and especially in case of low-grade energy sources. Thus, it has an indirect benefit on decreasing the environmental impacts of fossil fuels since it allows the extraction of extra amount of power by introducing it as a waste heat recovery system [39, 40]. Even though, heat recovery could be used without the installation of a ground-cooled condenser, the generated power

would be very limited due to the high ambient temperatures during the most hours of daytime. Therefore, the ground-cooled condenser takes advantage of the low ground temperature during the day allowing more effective working fluid expansion in the turbine. It was reported in Ref. [38] that the ground-cooled condenser can enhance the net output power of the cycle by 7.35%, 12.13% and 8.77% for R123, R124 and R245fa, respectively at an expander inlet pressure of 3 MPa.

This research aims to study the potential of shallow geothermal energy in Lebanon. The ground temperature was monitored in Bekaa-Lebanon (2020) and compared with the highest and lowest ambient air temperatures. The sensors of temperatures were placed at depths of 0.3 m, 0.6 m, 1 m, 1.3 m, 1.6 m, and 2 m underground. Based on the results of the experimental study, the system has been optimized, and the operating modes of the ground cooling system are then presented considering the effect of pressure drop in the heat exchangers.

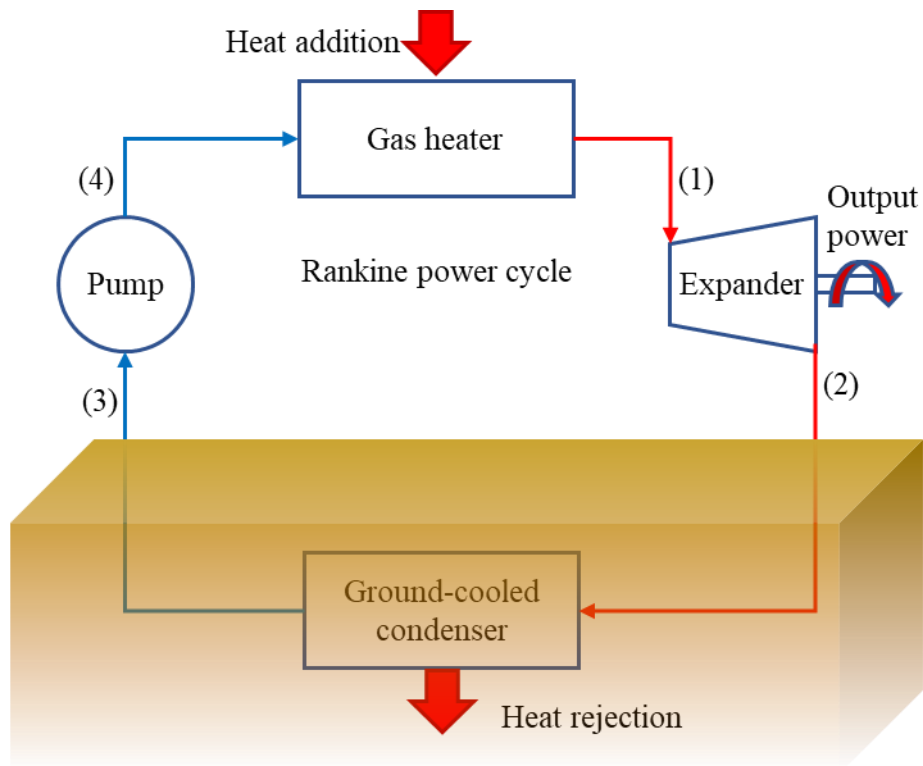


Figure 1: Rankine cycle combined with a ground-cooled condenser

2. Experimental setup

The setup used to measure the ground temperature is presented in Figure 2 including digital meter and thermocouples. The digital meter used has an accuracy of 0.5% of full-scale deflection as stated by the manufacturer and can measure a range of temperature between -9°C and 99°C , making it suitable for this experiment. It was a new device hence the calibration was provided by the manufacturer. Six thermocouples of type HT15T are inserted under the ground as shown in Figure 2. The measuring device has a fast response speed of 4.5 s with a low power consumption (less than 3 VA). It could be easily used as depicted in Figure 2. The thermocouples used have an error margin of ± 1 . It was also mentioned in the operation instructions of the digital panel meter that the best applicable temperature range is $0-50^{\circ}\text{C}$. This also makes the device more accurate in this experiment since the ground temperature in Bekaa-Lebanon is always within this range as will be presented in the next section. However, this accuracy is only valid for temperature measurements when the humidity is below 85%. Thus, it is decided to undertake the experiment in a place where the soil is dry all over the year, so not to compromise the accuracy of the results, especially for shallower ground temperatures. For this reason, the results obtained at a maximum depth of 2 m correspond to the most reliable collected data. To check further the reliability of the obtained results, the temperature variation was monitored precisely and especially during the winter season when raining. Accordingly, there was no significant variations in the corresponding values.

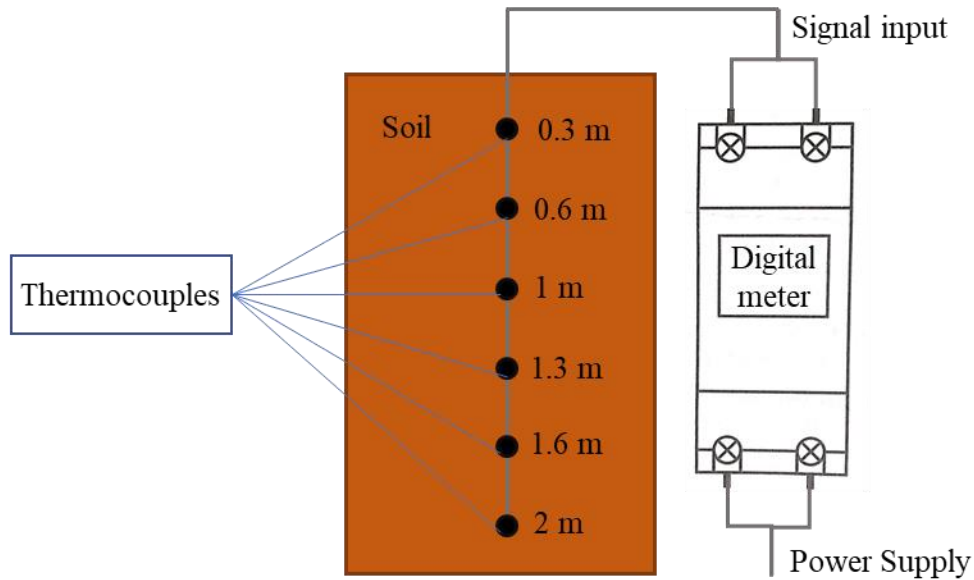


Figure 2: Schematic of the ground temperature measuring setup

3. Ground temperature measurement

Figure 3 shows the recorded ambient air and ground temperatures during 2020 in Bekaa-Lebanon. It can be seen that the ambient temperatures fluctuate significantly while the ground temperatures are considerably stable. As the depth increases the stability increases in which the curve corresponding to the depth of 2 m represents the least temperature fluctuations. During 2020, the maximum temperature difference at 2 m was 7°C since the temperature varied between 12°C and 19°C . This shows the great potential of using ground-cooled condenser in this location and mainly because the ground temperature is nearer to the lowest ambient temperature. Due to the stability recorded at 2 m, this depth will be considered as a reference for the ground temperature in the upcoming analyses.

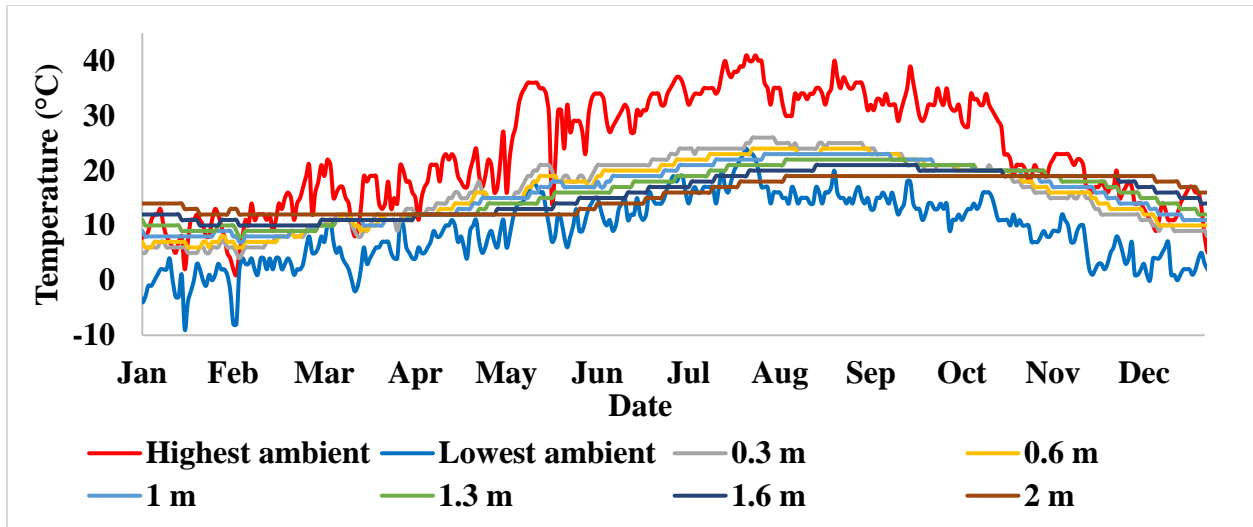


Figure 3: Ambient and ground temperature measurement in Bekaa-Lebanon during 2020

The ground temperatures in Bekaa are almost constant compared to the ambient air temperature due to the high fluctuations and temperature differences between ambient highest and lowest values during the day. This makes the use of shallow GE very important to reduce fluctuations in energy related systems because even at very shallow depths, the ground temperature is more stable than that of ambient air as shown in Figure 4. The results show that the annual average values of all ground temperatures are approximately equal to 15.5°C. This makes the results reliable revealing the effect of ground layers on each other which can be noticed from the different temperature variations all over the year but almost equal average temperatures.

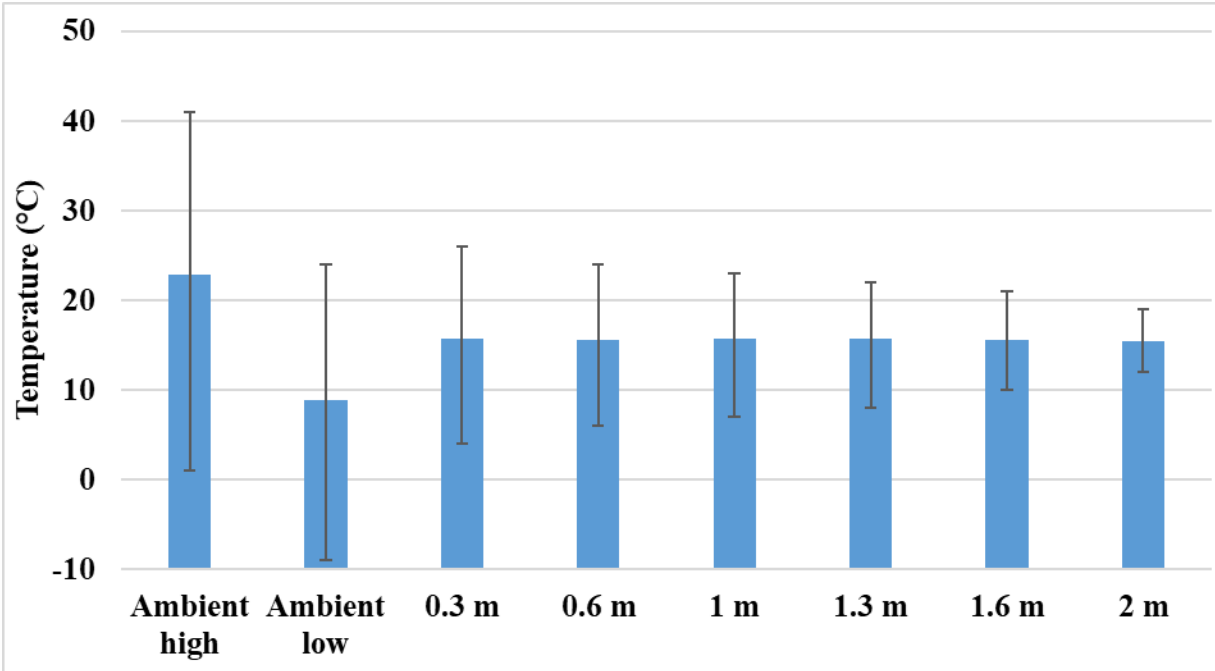


Figure 4: The difference between ambient and ground temperatures; average, highest, lowest and temperature difference in Bekaa-Lebanon during 2020

The highest, lowest, and average daily ambient air temperatures highly fluctuate compared to that of the ground at 2 m depth as shown in Figure 5, while the annual ground and ambient average temperatures are almost the same (15.5-16°C). However, it is essential to mention that this comparison is missing a crucial part which is that peak loads are usually reported during the daytime when the ambient temperature is relatively high. This makes the use of ground-cooled condenser very efficient for two main reasons that are stability and low temperature compared to that of ambient during operating hours. It is also expected that the ground temperature can be decreased using a cooling recovery strategy as will be presented in section 5.2 to enhance the performance of ground-cooled condenser during operation. Additionally, the peak load is not only the main reason for comparing the ground temperature with that of daytime ambient average temperature, but in many applications the system does not operate at night. This will be discussed in detail in section 5.3 showing the significance of choosing the operational duration of the proposed power cycle which is assumed to be from 06:00 to 24:00. Therefore, the upcoming

sections will be based on these assumption as if the system’s maximum possible operating duration is 18 hours/days.

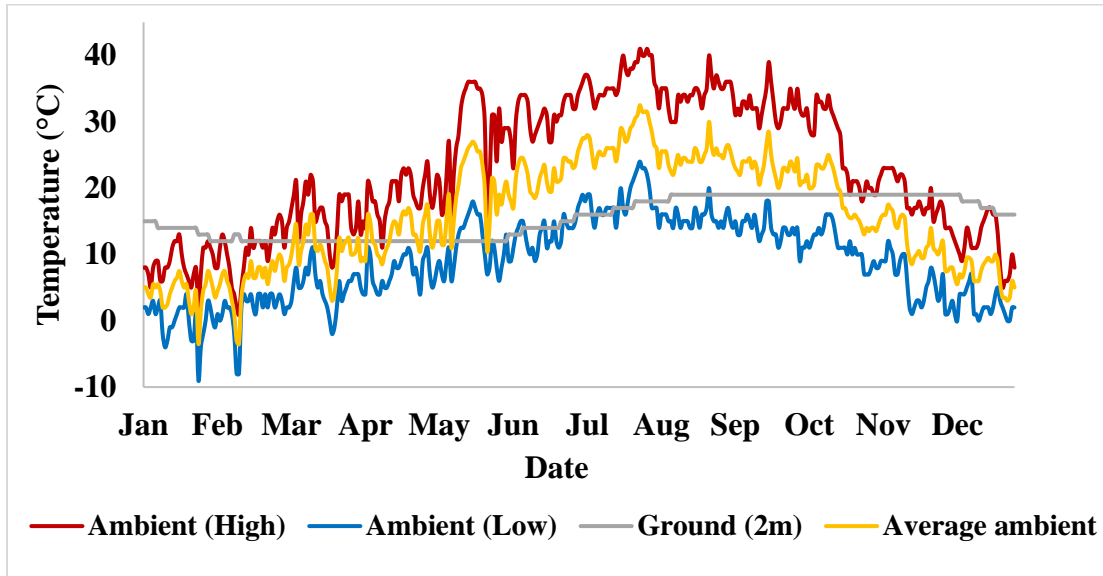


Figure 5: The variation of ambient highest, lowest, and average temperatures in comparison with the ground temperature at 2 m depth in Bekaa-Lebanon during 2020

4. Effective cooling source temperature

The aim of this section is to manage the operation of each condenser according to the lowest available temperature. This is essential because the aim of using a ground-cooled condenser is to decrease the condensation temperature in the Rankine power cycle knowing that this parameter is directly proportional to the cooling source temperature. As will be discussed in section 5.2, a hybrid-cooled condenser is used and composed of GHE and air/water-cooled heat rejector such that they utilize the ground and ambient air as cooling sources, respectively. This makes it necessary to control the operation of each cooling source subsystem by comparing the ground and ambient air temperatures at each instant during the day. This means that when the ground

temperature is lower than that of ambient, the GHE will be operating, otherwise the primary heat rejector will be the only functioning heat exchanger.

4.1 Operating cases

In this section, the ambient air temperature is assumed to be varying linearly during the day such that the lowest and highest ambient air temperatures are at 06:00 and 13:00, respectively. The equations and algorithm were coded into Visual Basic within Excel and used to carry out the simulation to estimate the value of daily effective cooling source temperature.

4.1.1 Case 1: Ground temperature is less than the lowest ambient temperature

This case occurs in summer when the ambient temperature is greater than that of ground during the entire day. Figure 6 presents a representation of case 1 such that the ground temperature horizontal line is always lower than that of ambient. In this case, the effective cooling source temperature during this day will be equal to that of the ground. This means that the GHE has the potential to operate from 06:00 to 24:00. However, this does not mean that the other heat rejector is not operating (see section 5.2). The primary heat rejector can remain functioning to reduce the heat rejected to the ground avoiding heat accumulation. In addition, the air/water cooled heat exchanger has an important role in such days since it will be running at night to ensure providing coolth compensation.

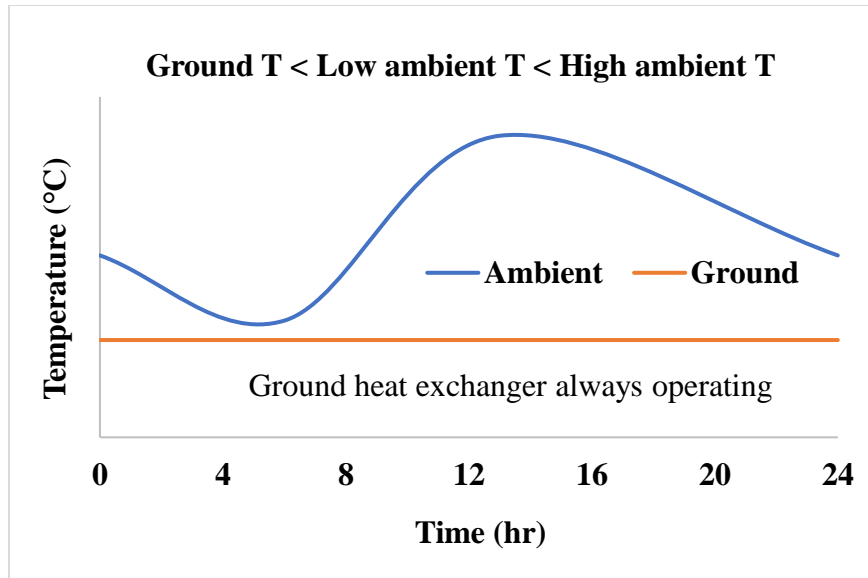


Figure 6: Ground cooling system operating the entire day (case 1)

4.1.2 Case 2: Ground temperature is higher than the highest ambient temperature

During winter, the ground temperature can be always higher than that of ambient air in some days as shown in Figure 3 and Figure 5 (mainly in January, February, and December). In such cases, it is needless to use the ground as a secondary cooling source since it is incapable of rejecting heat from water after passing through the primary heat rejector. Case 2 is depicted in Figure 7 in which the ground temperature at a depth of 2 m is greater than the highest ambient temperature. In this case, the condenser will be only depending on the air/water cooled heat exchanger since it is providing the lowest temperature during the entire operating duration. For this reason, the effective cooling source temperature in case 2 is equal to the average ambient temperature during operating hours. It is essential to mention that the possibility of having this case can be reduced after adopting the optimized system (see section 5.2). Therefore, it is expected that this case will be mainly representing the days where there is a sudden drop in the ambient air temperature.

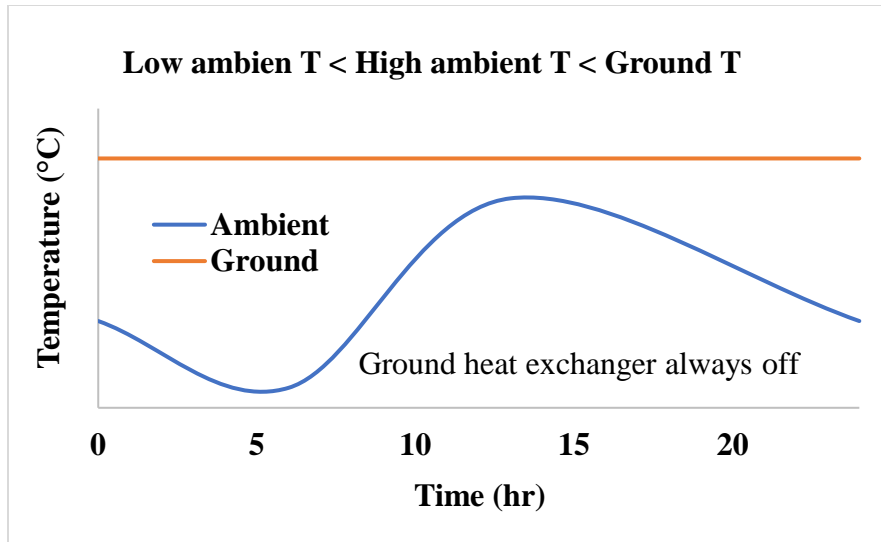


Figure 7: Ground cooling system not operating (case 2)

4.1.3 Case 3: The ambient temperature fluctuates around the ground temperature

This is the most complex case in which the ground temperature is lower than the highest ambient temperature while it is higher than that of lowest ambient. Figure 8 presents case 3 showing that the highest and lowest ambient temperatures are recorded at 06:00 and 13:00. As shown in Figure 3, this is the most frequently occurring case in the year 2020. Assuming that the ambient temperature is varying linearly during the day, the equation of a straight line is used to represent the temperature as shown in equation (1). The temperature function can be divided into two parts such that it is increasing during 06:00-13:00 and decreasing during 13:00-24:00. Thus, it is necessary to find the equations of these lines in terms of highest and lowest ambient, and ground

temperatures to calculate the daily effective cooling source temperature based on the ground cooling system (GCS) operating duration.

$$T = at + b \quad (1)$$

where T , a , t , and b are the temperature, slope, time, and y-intercept.

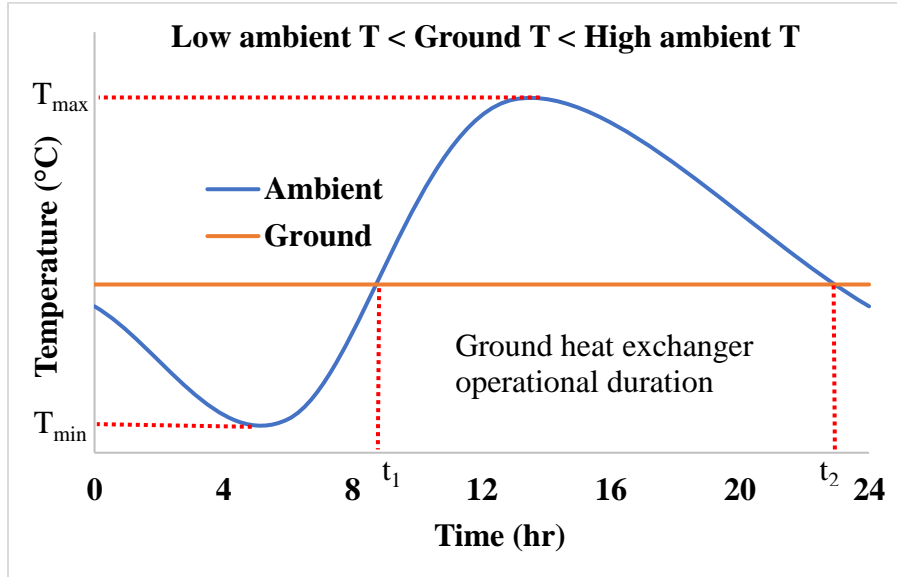


Figure 8: Ground cooling system partially operating (case 3)

Equation (2) shows the first intersection point between the ground and ambient temperatures.

$$t_1 = \frac{7(T_g - T_{min})}{T_{max} - T_{min}} + 6 \quad (2)$$

where T_{max} and T_{min} are the highest and lowest ambient temperatures during the day at 13:00 and 06:00, respectively. t_1 is the starting operation time of GCS and T_g is the ground temperature at a depth of 2 m. (Note: the value of t_1 must be between 06:00 and 13:00)

To calculate the approximate temperature at 24:00, the temperature is assumed to be decreasing linearly from 13:00 to the next day at 06:00. Therefore, if the temperature is decreasing at a constant rate, the temperature at 24:00 can be calculated as shown in equation (3).

$$T@24:00 = \frac{6(T_{max} - T_{min})}{17} + T_{min} \quad (3)$$

Equation (4) shows the second intersection point between the ground and ambient temperatures:

$$t_2 = \frac{17(T_{max} - T_g)}{T_{max} - T_{min}} + 13 \quad (4)$$

where t_2 corresponds to the second point of intersection between the ground and ambient temperature which is the time when the GCS is turned off. (Note: the value of t_2 must be between 13:00 and 24:00)

Figure 9 presents the effective cooling source temperature based on the model used for case 3 in which it shows that the GHE limits the increase in ambient temperature during the daytime. Equation (5) is used to calculate the average effective cooling source temperature during the days of case 3. For this reason, the area under the curve of Figure 9 is divided into three areas to apply easily the integration shown in equation (5). The area is divided into two trapezoids and one rectangle. Thus, equation (6) can be considered as a representation of the final approximate average temperature. (Note: this temperature must always be between the ground and lowest ambient temperatures)

$$T_{avg.eff} = \frac{\int_{t=6}^{t=24} T dt}{18} \quad (5)$$

$$T_{avg.eff} = \frac{(T_g + T_{min})(t_1 - 6) + 2T_g(t_2 - t_1) + (T_g + T@24:00)(24 - t_2)}{36} \quad (6)$$

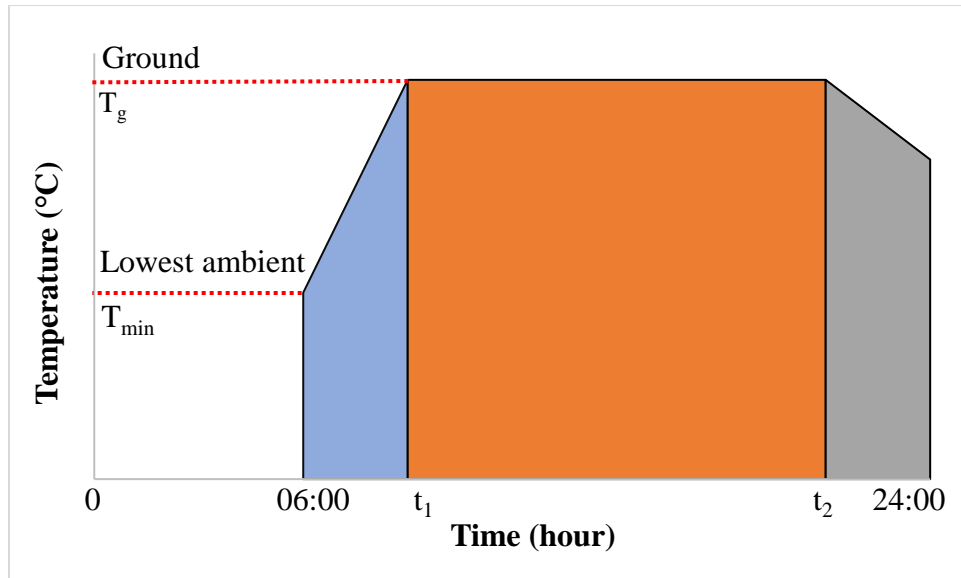


Figure 9: The effective cooling source temperature during a day representing case 3

4.2 Ambient vs. effective average temperatures

It is very important to calculate the daily average cooling source temperature since it directly affects the condensation temperature of working fluid. These temperatures have the same fluctuations during the year which is due to that they have a constant temperature difference (condenser's pinch temperature difference). Figure 10 shows the difference between average ambient and effective cooling source temperatures during 2020. The average ambient temperature is calculated considering the operating hours only (06:00-24:00) while that of effective is based on the cases presented in section 4.1. The results show that there is a significant difference between the two average temperatures and especially during summer. This confirms the contribution of ground cooling source to decrease the condensation temperature of the cycle. In some days of the year, the curves coincide representing case 2 where the ground temperature is always higher than that of ambient. In addition, the difference between the two curves almost represents the operating duration of the GCS.

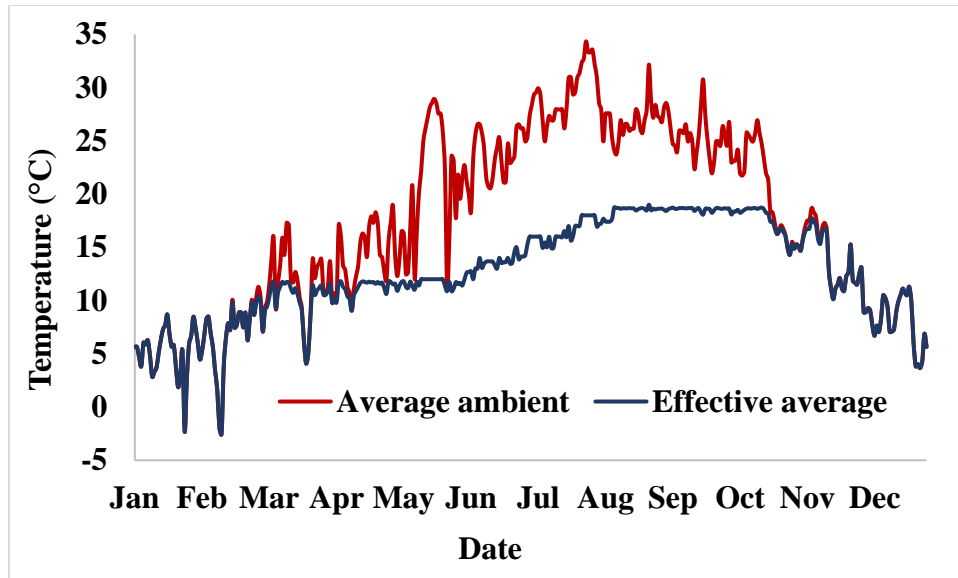


Figure 10: The variation of average ambient and effective cooling source temperatures in Bekaa-Lebanon during 2020

4.3 Ground cooling system operation

This section aims to present the daily and annual GCS operating durations. The maximum possible operating duration per day is assumed to be 18 hours (06:00 to 24:00). Thus, when the GCS can operate 18 hours, it will be reported as full operation (100%/day). Figure 11 shows the variation in the daily operating potential of GHE during 2020. It presents a great potential since the average operating duration is approximately 10 hours which represents 55.56% of the total operating time.

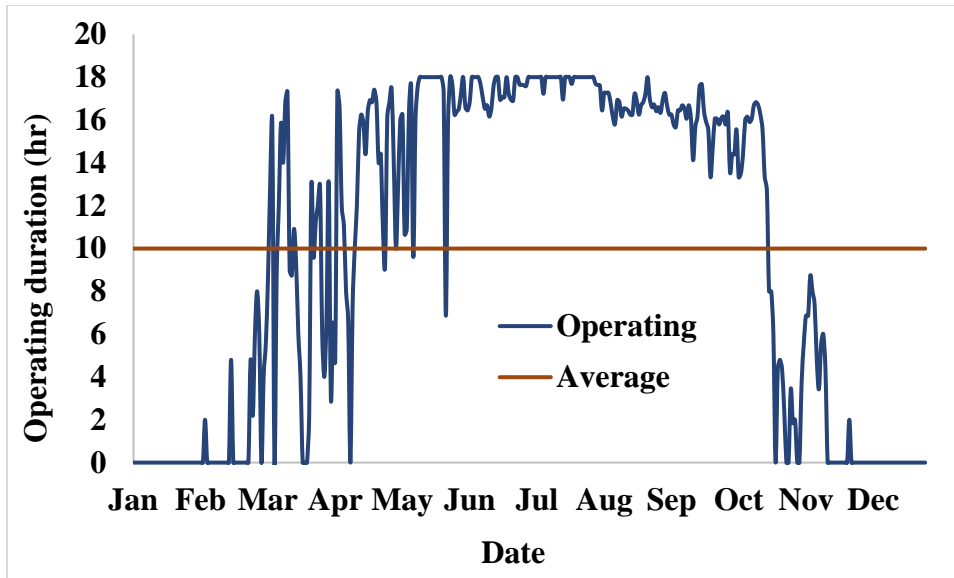


Figure 11: The estimated annual operating hours of ground cooling system

The results presented above have shown that the ground source can immensely decrease the condensation temperature of the power cycle. This is not only noticed from the difference between the temperatures, but also because the GCS can operate for long durations with large portions of the total operating time. Table 1 presents a detailed comparison between the ground and ambient sources regarding their differences in terms of temperatures and operations.

Table 1: The difference between the effect of ground and ambient cooling sources on the proposed system; operations and temperatures

Ground cooling system operation	Value	Unit
Maximum operating duration	18 (100)	hours/day (%)
Average operating duration	~10 (55.56)	hours/day (%)
Full operation (18 hours/day)	51 (13.97)	days/year (%)
Total operation (0-18 hours/day)	258 (70.68%)	days/year (%)

Maximum difference with highest ambient temperature	24	°C
Maximum difference with lowest ambient temperature	22	°C
Average difference with highest ambient temperature	7.33	°C
Average difference with lowest ambient temperature	6.64	°C

According to the operating cases presented in section 4.1, the GCS can be fully operating, partially operating, or turned off during the daytime. These possible operations refer to the cases 1, 2 and 3, respectively. Figure 12 shows the number of days for each case such that the GCS can be operating 258 days/year. However, 51 days of them correspond to full operations (18 hours/day). It is expected that the GCS can be turned off for 107 days/year, but it is essential to mention that the operating days can be more than 258 after adopting the optimized system (see section 5.2). Even though, the GCS is not operating during these 107 days, it is very important to take advantage of the cold ambient air in winter to recover the ground's coolth energy. This allows the ground source cooling system to operate more than 258 days/year considering the decrease in ground's temperature due to the additional heat rejection provided by the primary heat exchanger.

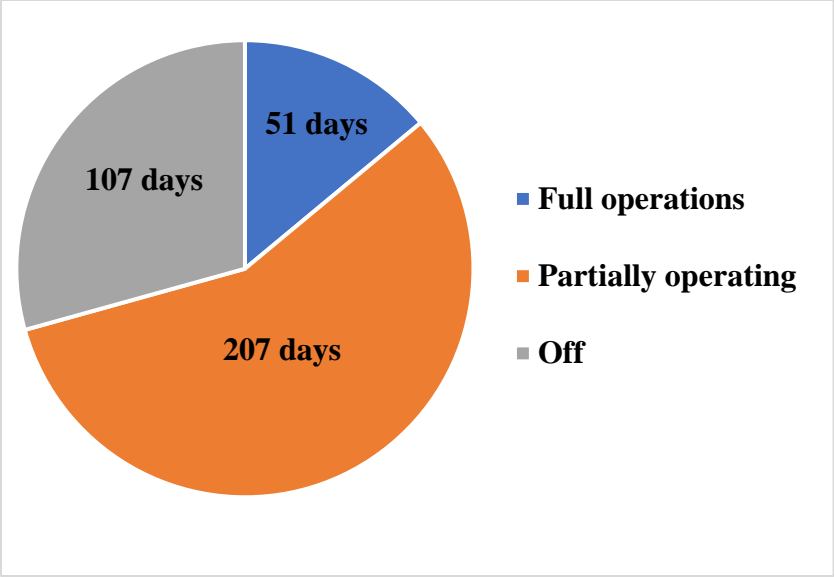


Figure 12: Summary of the potential of using a ground cooling system in Bekaa-Lebanon

5. Parametric study for system optimization

This section presents the methodology that is followed to optimize the power generation system incorporating a ground-cooled condenser, displayed in Figure 1. However, in this section, the ground heat exchanger is placed in soil considering the absence of shallow underground water in many regions (ex: Bekaa-Lebanon). System optimization also aims to mitigate the negative effects of critical parameters such as pressure drop, low mass flow rate and large ground loops. This requires the investigation of different configurations and working fluids to ascertain their effects on the performance of the system. The purpose of system optimization is to help increase the net output power whilst reducing the capital cost of installation (thermodynamic and economic aspects). Figure 13 presents the flow chart diagram displaying the optimization approach. The first part aims to compare two different possible ground cooling system's configurations based on the pressure drop inside the ground loop. After that, the operating modes will be presented depending on the cases displayed in section 4.1.

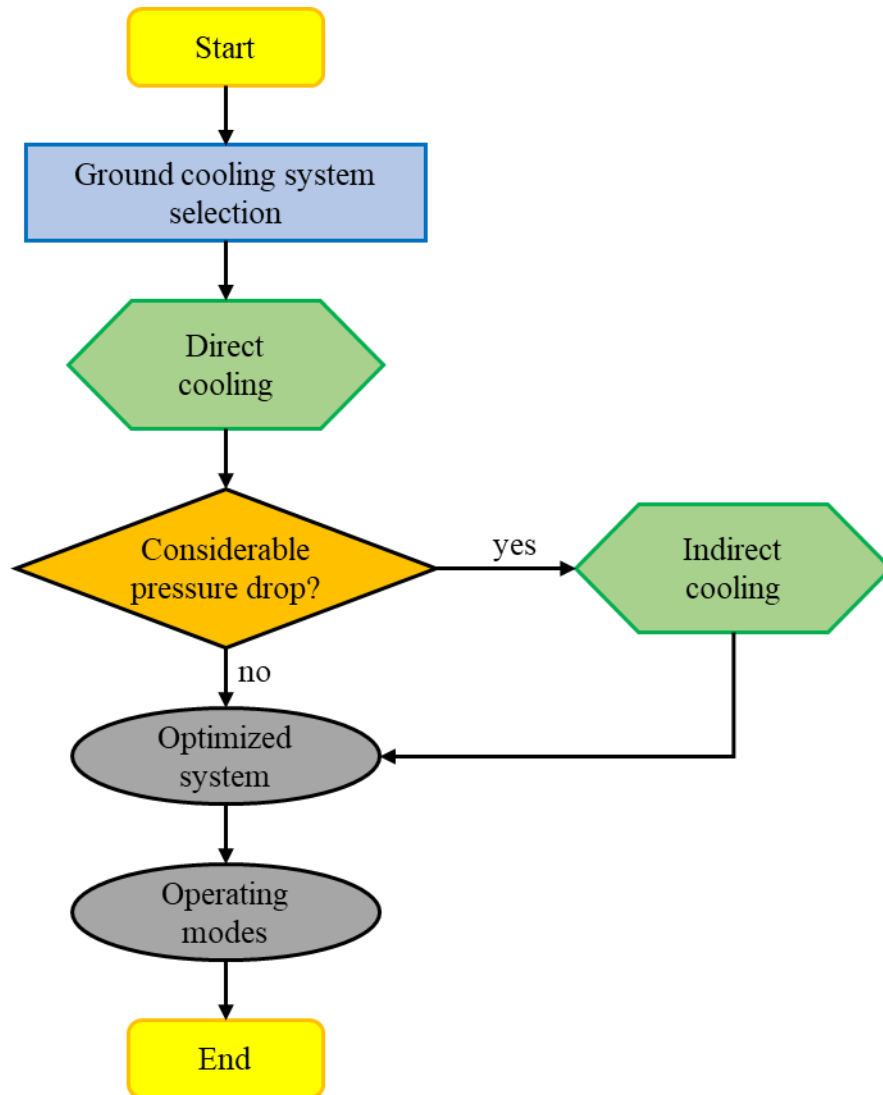
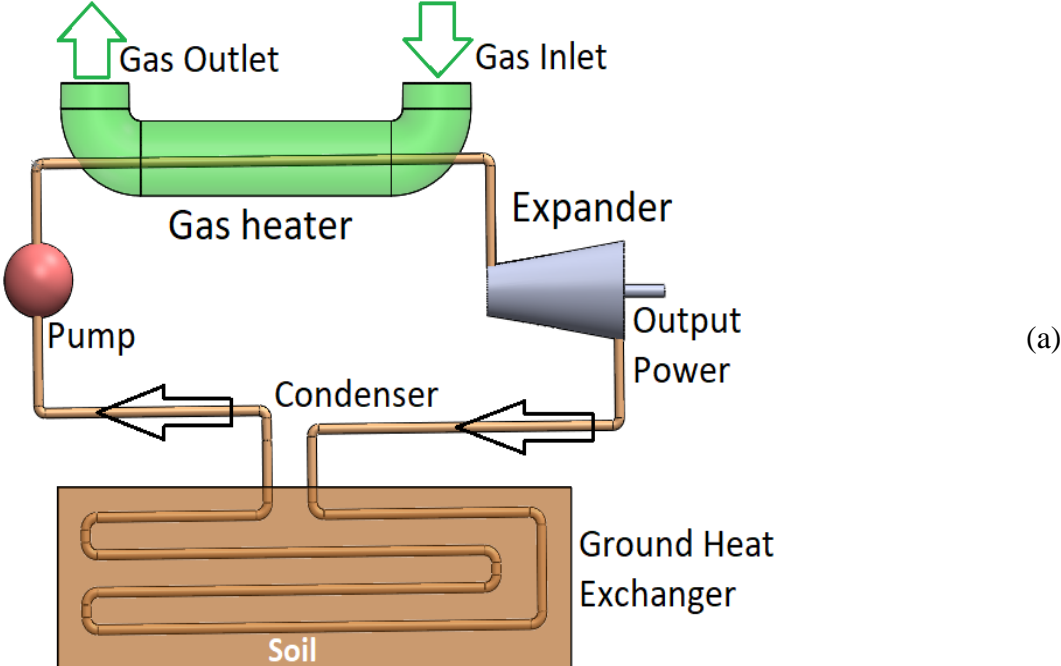


Figure 13: A flow chart diagram representing the methodology used in the current study

5.1 Direct cooling vs. indirect cooling

The system depicted in Figure 1 shows the ground-cooled condenser concept exhibiting a direct cooling method. This means that a direct contact between the cooling source and power cycle is available. This method is usually used to produce the highest amount of power since no intermediate loops are involved (minimum pinch temperature can be assumed). However, this may be accompanied by severe pressure drops in the condenser and hence negatively affecting the

overall system's performance. This is also more considerable in the absence of underground water when large ground loop is required. In most cases, the ground loop is installed in the soil as shown in Figure 14. The main concept of using shallow horizontal ground-cooled condenser as direct and indirect cooling systems is presented in Figure 14a and Figure 14b, respectively.



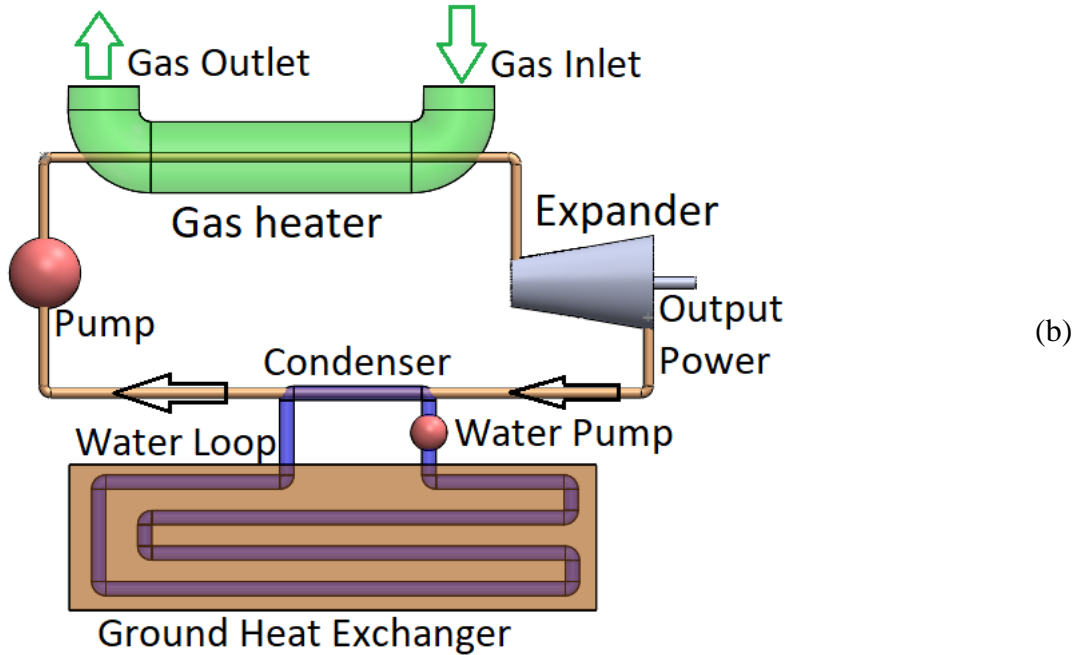


Figure 14: (a) Direct and (b) indirect ground cooling systems

5.1.1 Effect of pressure drop

This section aims to investigate the effect of pressure drop in the direct ground cooling system (see Figure 14a) to check if it is feasible to use such a strategy or it is better to add an intermediate loop to make the system more controllable and avoid the corresponding negative impacts.

Theory of modelling

The model used in this study is developed in Engineering Equation Solver (EES). The thermodynamic performance of the cycle depends mainly on the gas and power cycle's conditions (mass flow rate, temperatures, and pressures). The net output power can be calculated by:

$$\dot{W}_{net} = \dot{W}_t \cdot \eta_{ge} - \dot{W}_p - \Delta P \cdot Q \quad (7)$$

where \dot{W}_t is the turbine power, η_{ge} is the generator efficiency, \dot{W}_p is the pump power, ΔP is the pressure drop, and Q is the volumetric flow rate. \dot{W}_t and \dot{W}_p mainly depend on the mass flow rate of the working fluid and the enthalpy variation as shown in equations (8) and (9).

$$\dot{W}_t = \dot{m}_f(h_1 - h_2) \quad (8)$$

$$\dot{W}_p = \dot{m}_f(h_4 - h_3) \quad (9)$$

Equations (10) and (11) show the method used to ascertain the pressure drop effect [41]. This method is considered for turbulent flow in smooth pipes with values of Reynold's number ranging between 4000 and 10^5 .

$$f = \frac{0.316}{Re^{0.25}} \quad (10)$$

$$\Delta P = \frac{\rho \cdot f \cdot L \cdot v^2}{2D} \quad (11)$$

where f , Re , ΔP , ρ , L , v and D are friction coefficient, Reynold's number, pressure drop, density, length, velocity, and diameter, respectively. The working fluid's velocity is calculated as shown in equation (12).

$$v = \frac{4\dot{m}}{\rho \cdot \pi D^2} \quad (12)$$

Table 2 presents a summary of the conditions used for investigating the effect of pressure drop. These parameters are either fixed at the values mentioned in the table or will be varied and reported later during the simulations. According to a study carried out by Fujii *et al.* [42], it is recommended to keep the installed horizontal pipes 2 m apart to avoid thermal interference between them. This means that the effect of each pipe could reach 1 m. For this reason, in this section, the soil thermal

interference is assumed to be 1 m. In other words, the ground temperature is assumed to be constant at 1 m far from the GHE. The working fluid considered in this study is the same as that used in the reference system, i.e., CO₂-based transcritical Rankine cycle [37]. The cycle was used as a heat recovery system at the exhaust of an engine based on the study done by Shu *et al.* [43]. The exhaust gas was formed of 19.84% CO₂, 8.26% H₂O and 71.49% N₂. In the current work, the generator's efficiency was given a constant value of 90% which can be considered as an approximation same as that used in Ref. [43]. However, the generator's efficiency depends on the expander inlet and outlet temperatures.

Table 2: Parameters considered for investigating the effect of pressure drop

Parameters (Units)	Values
Gas heater diameter (mm)	40
Gas mass flow rate (kg/h)	300
Gas inlet temperature (°C)	777
Gas outlet temperature (°C)	120
Expander inlet pressure (MPa)	15
Expander inlet temperature (°C)	500
Ground temperature (°C)	15
Condensation temperature (°C)	25
Cycle pipe diameter (mm)	10

Expander isentropic efficiency	0.7
Pump isentropic efficiency	0.8
Generator efficiency	0.9

Methodology

The methodology that was followed to develop the presented model is as follows:

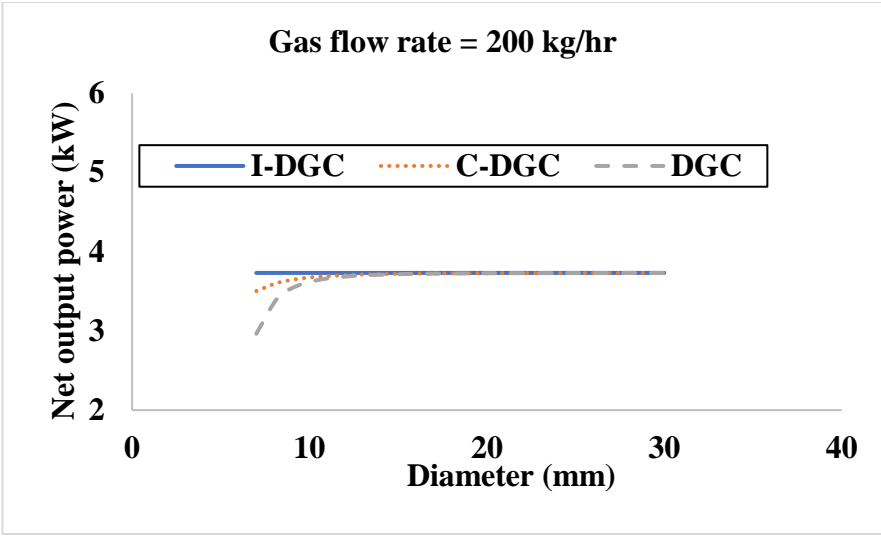
- Entering the heat source characteristics: composition, specific heat, thermal conductivity, viscosity, and Prandtl number.
- Choosing the condensation and evaporating temperatures based on the ground and heat source temperatures, respectively.
- Evaluating the enthalpy of working fluid at all states.
- Calculating the working fluid's mass flow rate.
- Dividing the heat exchangers (evaporator and condenser) into two parts to separate the change of phase and temperature investigations.
- Determining the working fluid's characteristics based on the average temperature in the two parts of heat exchangers: Reynolds number, Nusselt number, Prandtl number, viscosity, thermal conductivity, and convection heat transfer coefficient.
- Calculating the heat transfer coefficient of heating and cooling sources.
- Calculating the overall heat transfer coefficient (U) to evaluate the required size for both heat exchangers [37].
- Evaluating the pressure drop inside the heat exchangers.

- Calculating the cycle's net output power as shown in equation (7).

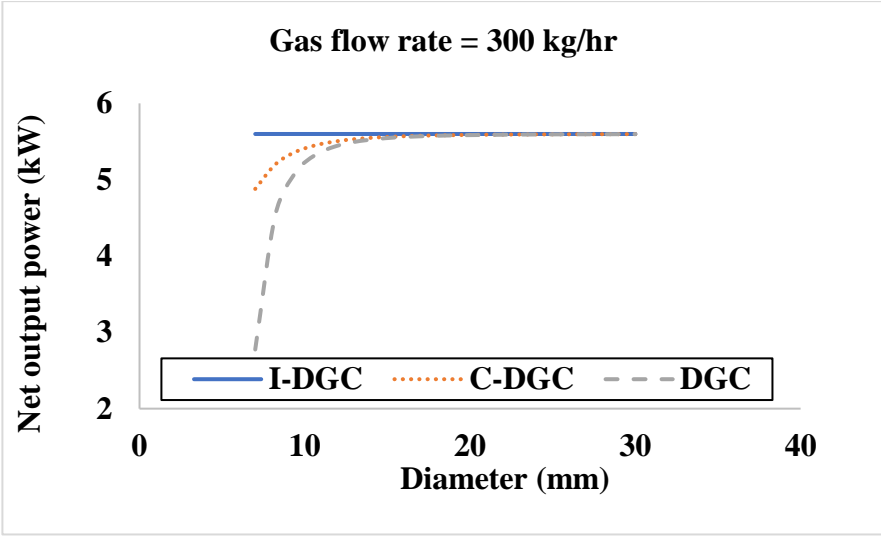
5.1.2 Results and discussion

In this section, the simulations are carried out to compare three models with minor differences; ideal direct ground cooling (I-DGC), considering pressure drop in the condenser (C-DGC) and considering pressure drop in both heat exchangers (DGC). The effect of pressure drop can be represented by the difference in net output power between the mentioned cases.

Figure 15 shows that the net output power is significantly affected by the cycle's pipe diameter. This is especially noticed at small pipe diameters (below 15 mm). However, the minimum value of diameter can also change depending on the grade of energy source since it was increased from ~13 to ~16 mm when the mass flow rate of gas increased from 200 to 300 kg/h. From this point of view, it can be reported that the negative effect of pressure drop can be avoided, but this depends on the available gas conditions and equipment cost that may be changed when large diameters are required.



(a)

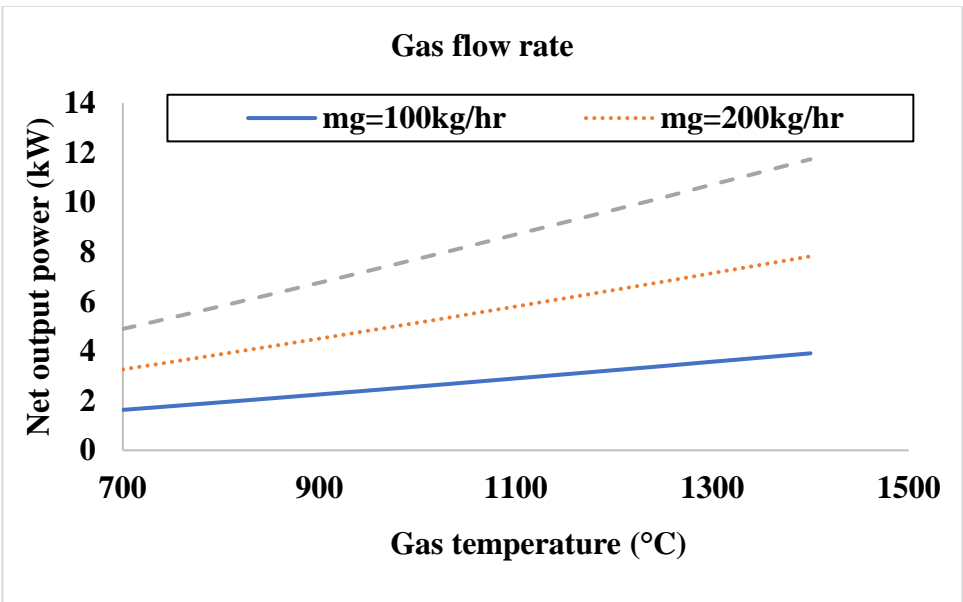


(b)

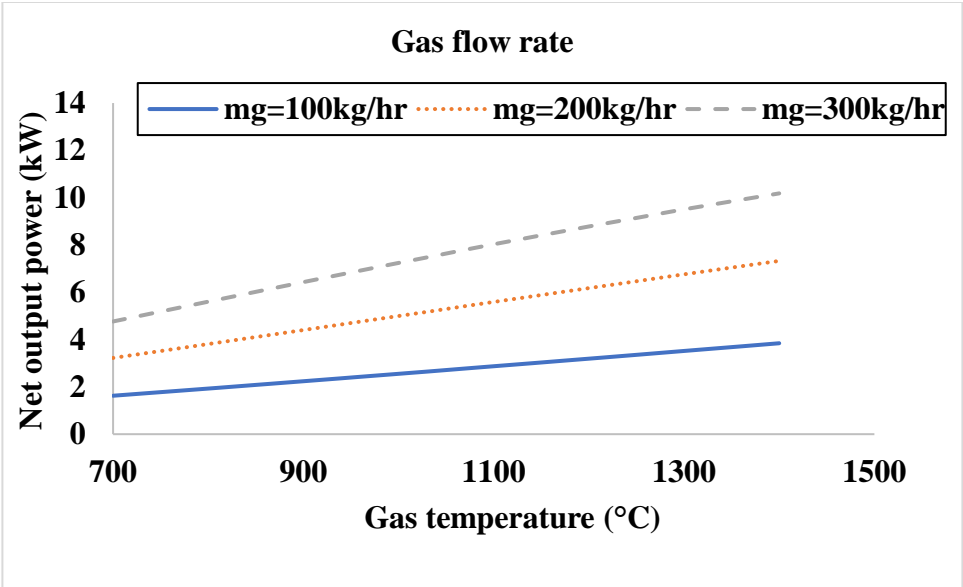
Figure 15: The effect of cycle's pipe diameter on the pressure loss at gas mass flow rates of (a) 200 kg/h and (b) 300 kg/h

To further study the effect of energy grade source on the pressure drop consideration, the gas temperature and mass flow rate were varied from 700 to 1500°C and 100 to 300 kg/h, respectively as shown in Figure 16. It can be noticed that the curves corresponding to the ideal case are diverging, while those of DGC are converging. This confirms that the pressure drop is relatively more considerable for higher grade energy sources. This shows that the pressure loss is

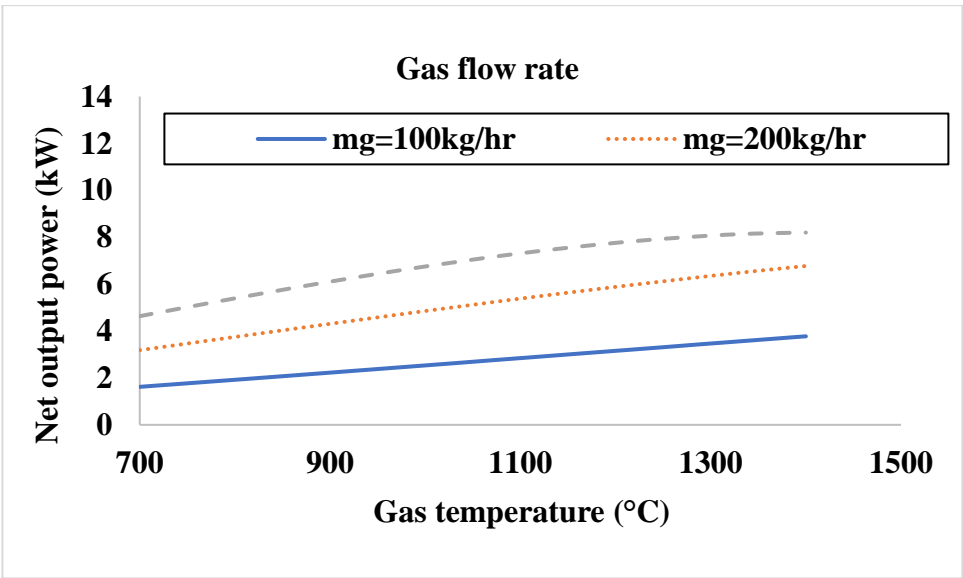
increasingly affected by the amount of heat added to the cycle. The pressure drop in both heat exchangers is almost the same which can be determined from the rate of change between the three presented models. The main reason causing the pressure loss effect to increase with the grade of energy is the increase of working fluid's mass flow rate. As shown in equation (5.2), the pressure drop is highly affected by the fluid's velocity knowing that the latter and mass flow rate are directly proportional at a given cross-sectional area.



(a)



(b)

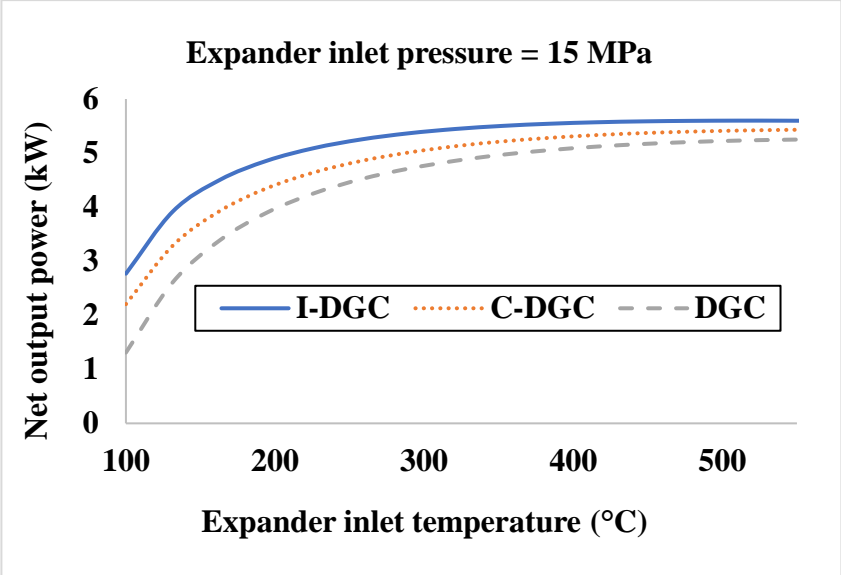


(c)

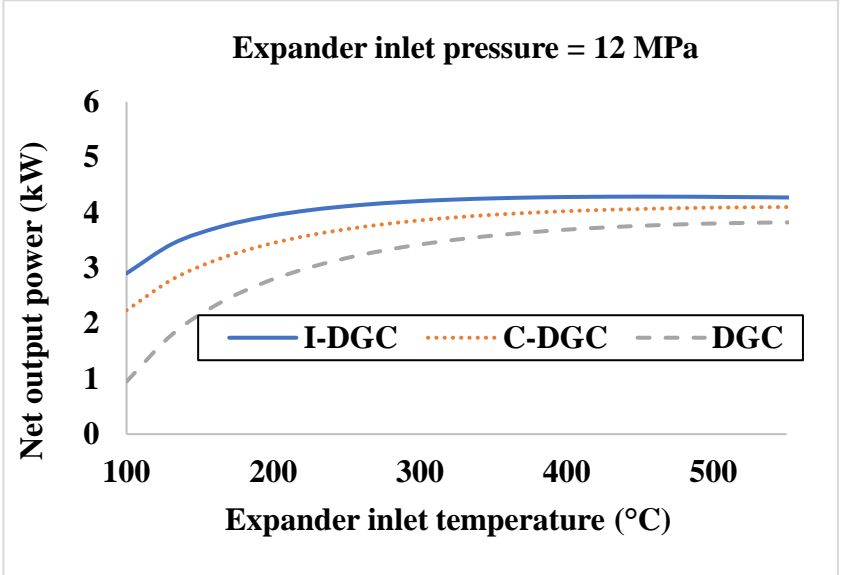
Figure 16: Effect of energy grade source on the net output power of (a) I-DGC, (b) C-DGC and (c) DGC

It may appear good in some cases to change the conditions of the cycle to optimize the system and achieve the best operating conditions. However, this is an ineffective method to avoid the negative impacts accompanied by pressure drop. This can be noticed from the results presented in Figure 17 since the change in expander inlet temperature and pressure did not significantly affect the

discrepancy between the studied models. Even though the net output power difference between the three considerations was decreased at high temperatures and pressures, this requires a considerable change in the conditions which is usually unacceptable.



(a)



(b)

Figure 17: The influence of expander inlet conditions on the effect of pressure drops at

(a) 15 MPa and (b) 12 MPa

The results presented in this section show that the effect of pressure drop cannot be neglected and will indeed cause significant drawbacks and change in cycle conditions. Thus, it would be recommended to introduce an intermediate water loop between the cycle and ground to ensure stability, make the system more controllable and avoid critical issues. This encourages using the indirect cooling strategy presented in Figure 14b. However, this system needs to be further modified to avoid a large ground loop installation. It is also important to mention that an antifreeze liquid must be mixed with water to avoid freezing since the cooling source temperature can decrease below 0°C as presented in Figure 10.

5.2 Optimized system

The heat rejected from a power cycle can be relatively massive with respect to the shallow GHE capacity, otherwise a large installation would be required. This causes additional expense making this system inappropriate for such utilizations. For this reason, it is better to integrate another cooling source into the hybrid power cycle such as air-cooled or water-cooled heat exchanger to operate as a primary heat rejector. Another advantage of this integration is to provide coolth compensation to the GHE in which this can immensely enhance its performance during operating hours. This recovery system can operate during the night whilst the ORC is off such that only the water loop will be running to transfer heat from the ground to the ambient air. However, it is recommended to introduce an underground storage medium that has high thermal conductivity and storage capacity, such as composite phase change materials, to allow the surrounding around the GHE to store coolth energy. This contributes to compensating the cooling ability of the ground source as well as improving the overall heat transfer coefficient to increase the heat transfer rate between the ground and circulating coolant.

The optimized system is presented in Figure 18 in which the two types of heat exchangers are connected in series. A bypass line is connected in parallel with the GHE to avoid exchanging heat with the ground when the ambient temperature is lower than that of the ground. On the other hand, the primary heat rejector will be always operating to reduce the amount of heat rejected from the cycle to the ground preventing heat accumulation and the need for large GHE installations. Therefore, a directional control valve (DCV) is used at the exit of primary heat rejector (state 6) to control the flow path of water; either passing through the GHE or overtaking it to directly enter the circulating pump. Another DCV is placed at state 8 to allow bypassing the cycle's condenser at night when the system is operating under recovery cooling mode. Thus, the two bypass lines help the ground to recover its coolth energy by decreasing its temperature when the power cycle is off (mainly at night) by extracting heat from the ground to the ambient air. It is also necessary to use a DCV at the inlet of primary heat rejector which helps overtaking this heat exchanger when the water exiting the condenser is below than that of ambient air (state 5).

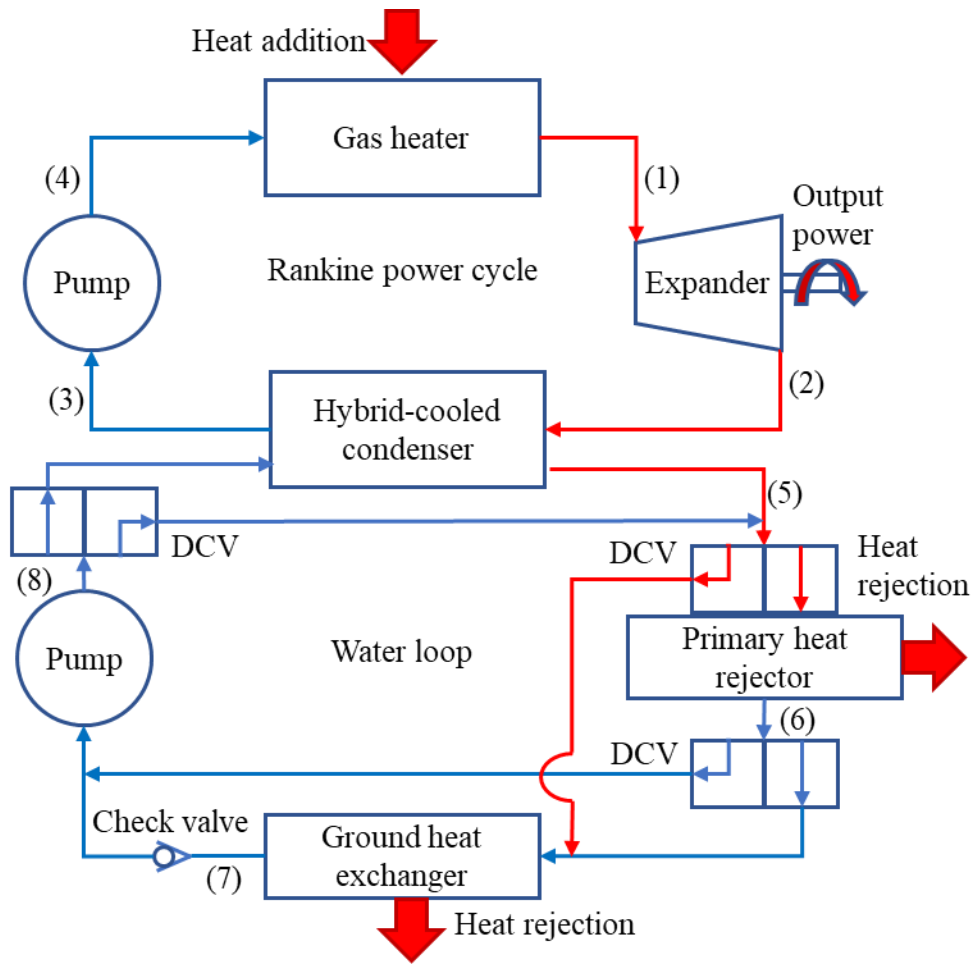


Figure 18: Schematic diagram of the optimized system; directional control valve (DCV)

The optimized system can be further enhanced by utilizing the heat rejected from the cycle between states 5 and 6 to increase the overall system's efficiency. This can maximize the output of the system by providing two types of outputs: electricity from the Rankine cycle and heat from the water loop. A large portion of heat is rejected from the water loop by the air/water-cooled heat exchanger, and this can be used to heat domestic water or utilized as an input to a heating system during winter months. Another possible utilization is the preheating of water prior to entering an electrolyzer. This can be helpful in producing hydrogen knowing that this type of combination suits the proposed system well since the electrolysis process requires both available forms of

energy, electrical and thermal. It is also possible to use a regenerator which is a heat exchanger used to transfer the heat remaining in the working fluid when exiting the expander to that entering the gas heater. This can also reduce the required heat input for producing the same amount of power or increase the net output power while maintaining constant heat addition.

5.3 Operating modes

This section aims to manage the operation of the optimized system presented in Figure 18. The DCVs placed at states 5, 6 and 8 are responsible for controlling the flow paths of the intermediate water loop, while the water pump helps regulating the amount of heat rejected from the cycle. Another advantage of the latter regulation is to facilitate the ground's coolth recovery at night. Concerning the operating modes, the ORC is either turned on or off, while the water loop has four operating modes with different flowing paths.

Normal operation (mode 1)

This mode corresponds to the case when the ground temperature is below that of the ambient air. For this reason, the coolant exiting the primary heat rejector (state 6) passes through the GHE to further decrease its temperature. Then, cold water (state 7) is supplied to the condenser (state 8) via a circulating pump. In this mode, there is no need to use any of the bypass lines since both heat rejectors are activated. This operation is usually required during the daytime when there is electricity demand, and the power cycle is turned on. However, it is essential to ensure that the ambient temperature during this mode is higher than that of the ground, otherwise the coolant entering the GHE will gain heat instead of rejecting it.

Ground cooling system turned off (mode 2)

The second possible mode of operation represents the case when the ground temperature is higher than that of the ambient air. This is also needed only when the power cycle is turned on, otherwise mode 4 will operate. The ground's temperature can be relatively high mainly in two cases, either in winter or due to high loads leading to heat accumulation. Thus, it is necessary to connect thermal sensors to allow regulatory control of the operating modes. The thermocouples must be placed very near to the GHE to detect the increase in effective ground's temperature and compare it with that of ambient. This regulation can significantly affect the cycle's performance since it helps to select the suitable operating mode (1 or 2).

Primary heat rejector turned off (mode 3)

In some summer days, the ambient air cannot be used to extract any amount of heat from the water loop due to the low water temperature exiting the condenser compared to that of ambient. In this case, it is better to bypass the primary heat rejector. Hot water directly enters the ground loop to decrease its temperature. In this mode, the ground cooling system (GCS) is operating at full load and the ground is receiving the highest amount of heat compared to other operating modes. In these periods, mode 4 is very essential during night hours to ensure coolth compensation because the condenser is only depending on the GCS during the daytime.

Coolth recovery (mode 4)

In this mode, the power cycle is turned off while water is only circulating in the primary heat rejector and GHE. This operation contributes to decreasing the ground's temperature by recovering its coolth energy. It helps to maintain low condensation temperatures and avoid ground heat accumulation. This mode is mainly used at night when the ground temperature is higher than that

of ambient. However, it can also be used during off-periods in some days of winter as presented in section 4.1. This operational mode shows the importance of integrating ground thermal energy storage technologies into the proposed optimized system. This means that introducing storage material in the form of grout can store coolth energy during night hours to increase the heat rejection capacity of the ground cooling system. This decreases the effective cooling source temperature during operation.

6. Conclusions

The ground and ambient temperatures were measured in Bekaa-Lebanon during 2020 and a detailed comparison was provided. The thermocouples were inserted at depths of 0.3, 0.6, 1, 1.3, 1.6 and 2 m. All ground temperatures were more stable than that of ambient air such that as the depth increased the stability increased. The maximum differences between highest and lowest temperatures during 2020 were 40°C, 33°C and 7°C for ambient high, ambient low and ground temperature at 2 m, respectively. The corresponding average values were 22.83°C, 8.87°C and 15.51°C. Three different operating cases were presented based on the difference between ground and ambient air temperatures in each day. According to these cases, the ground cooling system significantly decreased the average effective cooling source temperature. The ground cooling system can operate 207 days/year with full operations of 51 days. This was based on the potential of operating between 06:00 and 24:00 in which this was considered as the maximum duration since the ORC is always turned off during night hours. An intermediate water loop was added between the power cycle and GHE to avoid the negative effects of pressure drop. This was considered as indirect cooling strategy and mainly used to ensure stability and make the system more controllable. The condenser was further upgraded to a hybrid-cooled condenser which was based on ground and air/water heat exchangers. The latter was introduced as a primary heat rejector to

reduce the amount of heat rejected to the ground and provide coolth compensation during off-periods.

As for future work, the system can be further enhanced using a regenerator or investigating different types of working fluids. It is also necessary to study the economic feasibility of the proposed system by introducing it to a specific application. It would be recommended to integrate it into low-grade energy sources since it is expected that the proposed approach will have more influence on such systems. It is worth investigating more parameters that may affect the system's performance such as the ground soil thermal properties, soil type, water content, wind speed and rain fall. Additionally, the effect of cycle's conditions on the efficiency of components can be further studied to display more accurate results such as the generator and expander efficiencies.

References

- [1] Montaser Mahmoud, Mohamad Ramadan, Sumsun Naher, Keith Pullen, Abdul-Ghani Olabi, The impacts of different heating systems on the environment: A review, *Science of The Total Environment*, Volume 766, 2021, 142625, ISSN 0048-9697, <https://doi.org/10.1016/j.scitotenv.2020.142625>.
- [2] Yong Zhou, Yanfeng Liu, Dengjia Wang, Xiaojun Liu, Yingying Wang, A review on global solar radiation prediction with machine learning models in a comprehensive perspective, *Energy Conversion and Management*, Volume 235, 2021, 113960, ISSN 0196-8904, <https://doi.org/10.1016/j.enconman.2021.113960>.
- [3] Olga Tsvetkova, Taha B.M.J. Ouarda, A review of sensitivity analysis practices in wind resource assessment, *Energy Conversion and Management*, Volume 238, 2021, 114112, ISSN 0196-8904, <https://doi.org/10.1016/j.enconman.2021.114112>.
- [4] Montaser Mahmoud, Mohamad Ramadan, Abdul-Ghani Olabi, Keith Pullen, Sumsun Naher, A review of mechanical energy storage systems combined with wind and solar applications, *Energy Conversion and Management*, Volume 210, 2020, 112670, ISSN 0196-8904, <https://doi.org/10.1016/j.enconman.2020.112670>.
- [5] A.G. Olabi, C. Onumaegbu, Tabbi Wilberforce, Mohamad Ramadan, Mohammad Ali Abdelkareem, Abdul Hai Al – Alami, Critical review of energy storage systems, *Energy*, Volume 214, 2021, 118987, ISSN 0360-5442, <https://doi.org/10.1016/j.energy.2020.118987>.

- [6] Farayi Musharavati, Shoaib Khanmohammadi, Amirhossein Pakseresht, A novel multi-generation energy system based on geothermal energy source: Thermo-economic evaluation and optimization, *Energy Conversion and Management*, Volume 230, 2021, 113829, ISSN 0196-8904, <https://doi.org/10.1016/j.enconman.2021.113829>.
- [7] Víctor M. Ambriz-Díaz, Carlos Rubio-Maya, Oscar Chávez, Eduardo Ruiz-Casanova, Edgar Pastor-Martínez, Thermodynamic performance and economic feasibility of Kalina, Goswami and Organic Rankine Cycles coupled to a polygeneration plant using geothermal energy of low-grade temperature, *Energy Conversion and Management*, Volume 243, 2021, 114362, ISSN 0196-8904, <https://doi.org/10.1016/j.enconman.2021.114362>.
- [8] Antonio Rosato, Antonio Ciervo, Giovanni Ciampi, Michelangelo Scorpio, Francesco Guarino, Sergio Sibilio, Impact of solar field design and back-up technology on dynamic performance of a solar hybrid heating network integrated with a seasonal borehole thermal energy storage serving a small-scale residential district including plug-in electric vehicles, *Renewable Energy*, Volume 154, 2020, Pages 684-703, ISSN 0960-1481, <https://doi.org/10.1016/j.renene.2020.03.053>.
- [9] Fang Guo, Xudong Yang, Long-term performance simulation and sensitivity analysis of a large-scale seasonal borehole thermal energy storage system for industrial waste heat and solar energy, *Energy and Buildings*, Volume 236, 2021, 110768, ISSN 0378-7788, <https://doi.org/10.1016/j.enbuild.2021.110768>.
- [10] Rong Zeng, Xiaofeng Zhang, Yan Deng, Hongqiang Li, Guoqiang Zhang, Optimization and performance comparison of combined cooling, heating and power/ground source heat pump/photovoltaic/solar thermal system under different load ratio for two operation strategies, *Energy Conversion and Management*, Volume 208, 2020, 112579, ISSN 0196-8904, <https://doi.org/10.1016/j.enconman.2020.112579>.
- [11] Giti Nouri, Younes Noorollahi, Hossein Yousefi, Solar assisted ground source heat pump systems – A review, *Applied Thermal Engineering*, Volume 163, 2019, 114351, ISSN 1359-4311, <https://doi.org/10.1016/j.applthermaleng.2019.114351>.
- [12] Abdul Ghani Olabi, Montaser Mahmoud, Bassel Soudan, Tabbi Wilberforce, Mohamad Ramadan, Geothermal based hybrid energy systems, toward eco-friendly energy approaches, *Renewable Energy*, Volume 147, Part 1, 2020, Pages 2003-2012, ISSN 0960-1481, <https://doi.org/10.1016/j.renene.2019.09.140>.
- [13] Yuting He, Min Jia, Xiaogang Li, Zhaozhong Yang, Rui Song, Performance analysis of coaxial heat exchanger and heat-carrier fluid in medium-deep geothermal energy development, *Renewable Energy*, Volume 168, 2021, Pages 938-959, ISSN 0960-1481, <https://doi.org/10.1016/j.renene.2020.12.109>.
- [14] Koenraad F. Beckers, Amanda Kolker, Hannah Pauling, Joshua D McTigue, Devon Kesseli, Evaluating the feasibility of geothermal deep direct-use in the United States, *Energy Conversion and Management*, Volume 243, 2021, 114335, ISSN 0196-8904, <https://doi.org/10.1016/j.enconman.2021.114335>.

- [15] Juan C. Santamarta, Alejandro García-Gil, María del Cristo Expósito, Elías Casañas, Noelia Cruz-Pérez, Jesica Rodríguez-Martín, Miguel Mejías-Moreno, Gregor Götzl, Vasiliki Gemeni, The clean energy transition of heating and cooling in touristic infrastructures using shallow geothermal energy in the Canary Islands, *Renewable Energy*, Volume 171, 2021, Pages 505-515, ISSN 0960-1481, <https://doi.org/10.1016/j.renene.2021.02.105>.
- [16] Zhengxuan Liu, Mingjing Xie, Yuekuan Zhou, Yingdong He, Lei Zhang, Guoqiang Zhang, Dachuan Chen, A state-of-the-art review on shallow geothermal ventilation systems with thermal performance enhancement system classifications, advanced technologies and applications, *Energy and Built Environment*, 2021, ISSN 2666-1233, <https://doi.org/10.1016/j.enbenv.2021.10.003>.
- [17] Bayu Rudiyanto, IbnuAtho Illah, Nugroho Agung Pambudi, Chin-Chi Cheng, Reza Adiprana, Muhammad Imran, Lip Huat Saw, Renanto Handogo, Preliminary analysis of dry-steam geothermal power plant by employing exergy assessment: Case study in Kamojang geothermal power plant, Indonesia, *Case Studies in Thermal Engineering*, Volume 10, 2017, Pages 292-301, ISSN 2214-157X, <https://doi.org/10.1016/j.csite.2017.07.006>.
- [18] Elvira Buonocore, Laura Vanoli, Alberto Carotenuto, Sergio Ulgiati, Integrating life cycle assessment and emergy synthesis for the evaluation of a dry steam geothermal power plant in Italy, *Energy*, Volume 86, 2015, Pages 476-487, ISSN 0360-5442, <https://doi.org/10.1016/j.energy.2015.04.048>.
- [19] Khalid Altayib, Ibrahim Dincer, Development of a geothermal-flash organic Rankine cycle-based combined system with solar heat upgrade, *Energy Conversion and Management*, Volume 252, 2022, 115120, ISSN 0196-8904, <https://doi.org/10.1016/j.enconman.2021.115120>.
- [20] Guangli Fan, Yingjie Gao, Hamdi Ayed, Riadh Marzouki, Yashar Aryanfar, Fahd Jarad, Peixi Guo, Energy and exergy and economic (3E) analysis of a two-stage organic Rankine cycle for single flash geothermal power plant exhaust exergy recovery, *Case Studies in Thermal Engineering*, Volume 28, 2021, 101554, ISSN 2214-157X, <https://doi.org/10.1016/j.csite.2021.101554>.
- [21] Paweł Ziółkowski, Rafał Hyrzyński, Marcin Lemański, Bartosz Kraszewski, Sebastian Bykuć, Stanisław Głuch, Anna Sowizdzał, Leszek Pająk, Anna Wachowicz-Pyzik, Janusz Badur, Different design aspects of an Organic Rankine Cycle turbine for electricity production using a geothermal binary power plant, *Energy Conversion and Management*, Volume 246, 2021, 114672, ISSN 0196-8904, <https://doi.org/10.1016/j.enconman.2021.114672>.
- [22] Fatih Yilmaz, Murat Ozturk, Resat Selbas, Modeling and design of the new combined double-flash and binary geothermal power plant for multigeneration purposes; thermodynamic analysis, *International Journal of Hydrogen Energy*, 2021, ISSN 0360-3199, <https://doi.org/10.1016/j.ijhydene.2021.09.180>.
- [23] Montaser Mahmoud, Mohamad Ramadan, Sumsun Naher, Keith Pullen, Mohammad Ali Abdelkareem, Abdul-Ghani Olabi, A review of geothermal energy-driven hydrogen

- production systems, *Thermal Science and Engineering Progress*, Volume 22, 2021, 100854, ISSN 2451-9049, <https://doi.org/10.1016/j.tsep.2021.100854>.
- [24] Yunus Emre Yuksel, Murat Ozturk, Ibrahim Dincer, Development and assessment of a novel geothermal power-based multigenerational system with hydrogen and ammonia production options, *Energy Conversion and Management*, Volume 243, 2021, 114365, ISSN 0196-8904, <https://doi.org/10.1016/j.enconman.2021.114365>.
- [25] Gaosheng Wang, Xianzhi Song, Yu Shi, Rui Zheng, Jiacheng Li, Zhen Li, Production performance of a novel open loop geothermal system in a horizontal well, *Energy Conversion and Management*, Volume 206, 2020, 112478, ISSN 0196-8904, <https://doi.org/10.1016/j.enconman.2020.112478>.
- [26] Mariaines Di Dato, Claudia D'Angelo, Alessandro Casasso, Antonio Zarlunga, The impact of porous medium heterogeneity on the thermal feedback of open-loop shallow geothermal systems, *Journal of Hydrology*, Volume 604, 2022, 127205, ISSN 0022-1694, <https://doi.org/10.1016/j.jhydrol.2021.127205>.
- [27] Ahmed A. Serageldin, Ali Radwan, Takao Katsura, Yoshitaka Sakata, Shigeyuki Nagasaka, Katsunori Nagano, Parametric analysis, response surface, sensitivity analysis, and optimization of a novel spiral-double ground heat exchanger, *Energy Conversion and Management*, Volume 240, 2021, 114251, ISSN 0196-8904, <https://doi.org/10.1016/j.enconman.2021.114251>.
- [28] Bin Liang, Meiqian Chen, Yasin Orooji, Effective parameters on the performance of ground heat exchangers: A review of latest advances, *Geothermics*, Volume 98, 2022, 102283, ISSN 0375-6505, <https://doi.org/10.1016/j.geothermics.2021.102283>.
- [29] Michal Chwieduk, New global thermal numerical model of vertical U-tube ground heat exchanger, *Renewable Energy*, Volume 168, 2021, Pages 343-352, ISSN 0960-1481, <https://doi.org/10.1016/j.renene.2020.12.069>.
- [30] Mohammadamin Ahmadfard, Michel Bernier, A review of vertical ground heat exchanger sizing tools including an inter-model comparison, *Renewable and Sustainable Energy Reviews*, Volume 110, 2019, Pages 247-265, ISSN 1364-0321, <https://doi.org/10.1016/j.rser.2019.04.045>.
- [31] Ali Sedaghat, Mohammad Habibi, Ali Hakkaki-Fard, A novel ground thermal recovery system for horizontal ground heat exchangers in a hot climate, *Energy Conversion and Management*, Volume 224, 2020, 113350, ISSN 0196-8904, <https://doi.org/10.1016/j.enconman.2020.113350>.
- [32] A.M. Bulmez, V. Ciofoaia, G. Năstase, G. Dragomir, A.I. Brezeanu, A. Şerban, An experimental work on the performance of a solar-assisted ground-coupled heat pump using a horizontal ground heat exchanger, *Renewable Energy*, Volume 183, 2022, Pages 849-865, ISSN 0960-1481, <https://doi.org/10.1016/j.renene.2021.11.064>.

- [33] Marwa Dabaieh, Ahmed A. Serageldin, Earth air heat exchanger, Trombe wall and green wall for passive heating and cooling in premium passive refugee house in Sweden, *Energy Conversion and Management*, Volume 209, 2020, 112555, ISSN 0196-8904, <https://doi.org/10.1016/j.enconman.2020.112555>.
- [34] Giouli Mihalakakou, Manolis Souliotis, Maria Papadaki, George Halkos, John Paravantis, Sofoklis Makridis, Spiros Papaefthimiou, Applications of earth-to-air heat exchangers: A holistic review, *Renewable and Sustainable Energy Reviews*, 2021, 111921, ISSN 1364-0321, <https://doi.org/10.1016/j.rser.2021.111921>.
- [35] Saeid Mohammadzadeh Bina, Hikari Fujii, Shunsuke Tsuya, Hiroyuki Kosukegawa, Comparative study of hybrid ground source heat pump in cooling and heating dominant climates, *Energy Conversion and Management*, Volume 252, 2022, 115122, ISSN 0196-8904, <https://doi.org/10.1016/j.enconman.2021.115122>.
- [36] Sarah Noye, Rubén Mulero Martinez, Laura Carnieletto, Michele De Carli, Amaia Castelruiz Aguirre, A review of advanced ground source heat pump control: Artificial intelligence for autonomous and adaptive control, *Renewable and Sustainable Energy Reviews*, Volume 153, 2022, 111685, ISSN 1364-0321, <https://doi.org/10.1016/j.rser.2021.111685>.
- [37] Montaser Mahmoud, Mohamad Ramadan, Sumsun Naher, Keith Pullen, Abdul-Ghani Olabi, CO₂ – Based transcritical Rankine cycle coupled with a ground-cooled condenser, *Thermal Science and Engineering Progress*, Volume 25, 2021, 100948, ISSN 2451-9049, <https://doi.org/10.1016/j.tsep.2021.100948>.
- [38] Montaser Mahmoud, Mohammad Alkhedher, Mohamad Ramadan, Sumsun Naher, Keith Pullen, An investigation on organic Rankine cycle incorporating a ground-cooled condenser: Working fluid selection and regeneration, *Energy*, Volume 249, 2022, 123742, ISSN 0360-5442, <https://doi.org/10.1016/j.energy.2022.123742>.
- [39] Montaser Mahmoud, Mohamad Ramadan, Keith Pullen, Mohammad A. Abdelkareem, Tabbi Wilberforce, Abdul-Ghani Olabi, Sumsun Naher, Waste Heat Recovery Applications Incorporating Phase Change Materials, *Encyclopedia of Smart Materials*, Elsevier, 2022, Pages 513-521, ISBN 9780128157336, <https://doi.org/10.1016/B978-0-12-815732-9.00074-7>.
- [40] Anurag Kumar, Dibakar Rakshit, A critical review on waste heat recovery utilization with special focus on Organic Rankine Cycle applications, *Cleaner Engineering and Technology*, Volume 5, 2021, 100292, ISSN 2666-7908, <https://doi.org/10.1016/j.clet.2021.100292>.
- [41] Robert W. Fox, Alan T. McDonald, Philip J. Pritchard, *Introduction to Fluid Mechanics*, 6e, Wiley, 2003.
- [42] Hikari Fujii, Keita Nishi, Yoshihito Komaniwa, Naokatsu Chou, Numerical modeling of slinky-coil horizontal ground heat exchangers, *Geothermics*, Volume 41, 2012, Pages 55-62, ISSN 0375-6505, <https://doi.org/10.1016/j.geothermics.2011.09.002>.

- [43] Gequn Shu, Lingfeng Shi, Hua Tian, Shuai Deng, Xiaoya Li, Liwen Chang, Configurations selection maps of CO₂-based transcritical Rankine cycle (CTRC) for thermal energy management of engine waste heat, *Applied Energy*, Volume 186, Part 3, 2017, Pages 423-435, ISSN 0306-2619, <https://doi.org/10.1016/j.apenergy.2016.03.049>.